Bio-plausible Neuromorphic Disturbance Observer Based on Emulation Theory: Extended Version

Hongfu Xu, Xiaoyu Guo, *Member, IEEE*, Shengbo Wang and Shuo Gao, *Senior Member, IEEE*,

***Abstract*—Biological neural systems achieve remarkable robustness and adaptability in uncertain environments through sparse, event-driven spike-based information processing and adaptive regulation. Inspired by this paradigm, this paper develops a neuromorhpic disturbance observer (NDO) and control framework that replaces conventional continuous-time signal representations with spike-timing encoding. Both disturbance estimates and control inputs are constructed via integrate-and-fire (IF) neuron dynamics from discrete spike events, yielding intrinsically event-driven updates. An adaptive-threshold triggering mechanism is inspired by spike-frequency adaptation (SFA), enabling history-dependent regulation of spike generation. Simulation results demonstrate that the proposed framework achieves neurally inspired robustness and adaptability, while the adaptive-threshold spiking scheme reduces spike events to 42.6% of the fixed-threshold case under noisy conditions.**

***Index Terms*—Spike-based, neuromorphic disturbance observer, adaptive and robust.**

I. Introduction

Biological neural systems exhibit remarkable robustness and adaptability in complex and uncertain environments, achieved through sparse spiking activity, event-driven information processing, and spike-frequency adaptation (SFA) mechanisms, where firing thresholds dynamically adjust based on neural activity history [1]–[3]. This spike-timing-based paradigm enables stable yet flexible motor behaviors under pervasive uncertainty. The sparse and adaptive nature of spike-based computation endows neural systems with inherent robustness to noise and perturbations, providing a compelling blueprint for designing control systems that remain low-power and reliable under uncertainty. Motivated by this, increasing efforts have sought to incorporate neurally inspired mechanisms into engineering control systems to enhance closed-loop robustness [4], [5].

Existing studies have focused on designing controllers that integrate neural dynamics with spiking output mechanisms while providing stability guarantees [6]–[8]. Among these, Petri et al. [6] proposed an emulation-based approach that offers formal stability guarantees for neuromorphic controllers. However, such works are typically developed under idealized disturbance-free assumptions and overlook SFA in the neural dynamics.

To address these limitations, this paper proposes a bio-plausible controller, in which both disturbance estimates and control inputs are represented as spike timing sequences generated via integrate-and-fire (IF) dynamics [9]. We develop a composite feedforward–feedback control structure driven by a neuromorphic disturbance observer (NDO), which extends classical disturbance observer (DO) theory [10], [11] to neuromorphic spike-based control systems. Moreover, motivated by SFA in neuronal firing threshold dynamics [1], [12], an adaptive-threshold triggering mechanism is introduced to regulate spike generation based on firing history: frequent spiking increases the threshold, whereas prolonged silence decreases it. This history-dependent regulation enables spike emission to adaptively track disturbances without prior knowledge, thereby achieving neurally inspired robustness and adaptability in closed-loop control.

Based on the considerations above, the main contributions of this paper are summarized as follows:

1) Inspired by IF neuron, a neurally inspired disturbance estimation and control paradigm is proposed, incorporating an adaptive-threshold triggering rule inspired by the SFA mechanisms.
2) For systems subject to external disturbances, the closed-loop stability of the NDO and control scheme is rigorously established via emulation theory. This framework is further extended to multiple-input multiple-output (MIMO) LTI systems.
3) Numerical simulations validate the NDO achieves accurate disturbance estimation, while demonstrating robustness and adaptability under external disturbances. Furthermore, under noisy conditions, the adaptive-threshold spiking scheme reduces spike events to 42.6% of the fixed-threshold case while maintaining comparable disturbance estimation accuracy.

II. PRELIMINARIES

The set of real numbers is denoted by $\mathbb{R}$, while we define $\mathbb{R}_{\geq 0} := [0, +\infty)$ and $\mathbb{R}_{>0} := (0, +\infty)$. Similarly, $\mathbb{Z}$ represents the integers, with $\mathbb{Z}_{\geq 0} := \{0, 1, 2, \ldots\}$ and $\mathbb{Z}_{>0} := \{1, 2, \ldots\}$. For a function $f\colon \mathbb{R} \to \mathbb{R}$, its right-hand and left-hand limits at $t \in \mathbb{R}$ are denoted by $f(t^+) = \lim_{s \downarrow t} f(s)$ and $f(t^-) = \lim_{s \uparrow t} f(s)$, respectively. The induced 2-norm of a

Hongfu Xu is with the School of Automation Science and Electrical Engineering, Beihang University, Beijing 100191, China (e-mail: hongfuxu@buaa.edu.cn).

Xiaoyu Guo is with the Department of Mechanical Engineering, City University of Hong Kong, Hong Kong (e-mail: xiaoyguo@cityu.edu.hk).

Shengbo Wang is with the Department of Electrical and Electronic Engineering, The University of Hong Kong, Hong Kong (e-mail: shengbo_wang@connect.hku.hk).

Shuo Gao is with the School of Instrumentation and Optoelectronic Engineering, Beihang University, Beijing 100191, China (e-mail:shuo_gao@buaa.edu.cn).

This work is an extended version of the paper submitted to the International Conference on Automation and Computing (ICAC) 2026. This version provides detailed proofs as well as extensions to nonlinear systems.

vector $x \in \mathbb{R}^{n_x}$ is written as $\|x\|$. Given a set $\mathcal{Y} \subset \mathbb{R}^{n_y}$ ($n_y \in \mathbb{Z}_{>0}$), $\mathcal{L}_\infty(\mathcal{Y})$ denotes the set of Lebesgue measurable and locally essentially bounded functions $y\colon \mathbb{R}_+ \to \mathcal{Y}$. The Dirac delta distribution δ satisfies $\delta(t) = 0$ for $t \neq 0$ and $\int_{-\infty}^{\infty} \delta(t)\,dt = 1$. $m \in \{y, \hat{y}\}$. Finally, we define the norm $\|v\|_\star = \sup_{t\in\mathbb{R}_{\geq 0}} |\int_0^t v(s)ds|$.

III. Approximation Properties of Spike System

The control problem for a linear time-invariant (LTI) system described by

$$\dot{x} = Ax + Bu + d, \qquad y = Cx, \tag{1}$$

where $x \in \mathbb{R}^{n_x}$ denotes the state vector with initial condition $x(0) = x_0 \in \mathbb{R}^{n_x}$, $y \in \mathbb{R}^{n_y}$ is the output, and $u \in \mathbb{R}^{n_u}$ represents the (spiking) control input, d denotes the time-varying disturbance. $A \in \mathbb{R}^{n_x\times n_x}$, $B \in \mathbb{R}^{n_x\times n_u}$, $C \in \mathbb{R}^{n_y\times n_x}$. Here, n_x, n_y, and n_u are positive integers. The following assumption is adopted.

Assumption 1. There exists a matrix $K \in \mathbb{R}^{n_y\times n_u}$ such that the matrix $A + BKC$ is Hurwitz.

Assumption 2. The disturbance $d(t)$ is continuously differentiable and its derivative is bounded, i.e., there is a known constant $\delta > 0$ such that $\|\dot{d}(t)\| \leq \delta$ for $t \geq 0$.

Assumption 3. There exists a matrix $L \in \mathbb{R}^{n_y\times n_u}$ such that the matrix $A + LC$ is Hurwitz.

Define the augmented state $z = \begin{bmatrix} x, d \end{bmatrix}^T$, and construct the extended system

$$\dot{z} = A_d z + B_d u + [0, \dot{d}]^\top,\ y = C_d z$$

where $A_d = \begin{bmatrix} A & I \\ 0 & 0 \end{bmatrix}$, $B_d = \begin{bmatrix} B \\ 0 \end{bmatrix}$, $C_d = \begin{bmatrix} C & 0 \end{bmatrix}$.

Let $\hat{z} = [\hat{x}, \hat{d}]^T$, the ESO is designed as

$$\dot{\hat{z}} = A_d\hat{z} + B_d u + L\big(y - \hat{y}\big),\ \hat{y} = C_d\hat{z} \tag{2}$$

Define the estimation error $e = z - \hat{z}$. Then, the error dynamics satisfy $\dot{e} = (A_d - LC_d)e + [0, \dot{d}]^\top$. If Assumption 3 is satisfied, the estimation error satisfies

$$\|e_x(t)\| \leq M_e e^{-\lambda t}\|e_x(0)\| + \gamma \sup_{0\leq s\leq t} \|\dot{d}(s)\|, \tag{3}$$

where $M_e > 0$, $\lambda > 0$, and $\gamma > 0$ are positive constants.

To facilitate the analysis, we first consider a single-input single-output (SISO) system. The disturbance estimation and control architecture is illustrated in Fig. 1, where the disturbance estimate $\hat{d}$ is generated by a neuromorphic estimator composed of 4 neurons, and the control input $u_{\rm fb}$ is produced by a neuromorphic controller consisting of 2 neurons. The underlying dynamics are inspired by the integrate-and-fire neuron model. Consider the following dynamics between four spiking actions:

$$\frac{d}{dt}\eta_{y,\ell}(t) = \max\{0, (3-2\ell)y(t)\}, t \in [t_{y_\ell,i_1}, t_{y,i_1+1}), \tag{4a}$$

$$\frac{d}{dt}\eta_{\hat{y},\ell}(t) = \max\{0, (3-2\ell)\hat{y}(t)\}, t \in [t_{\hat{y}_\ell,i_1}, t_{\hat{y},i_1+1}) \tag{4b}$$

where $t_{y_\ell,0} = t_{\hat{y}_\ell,0} = 0$ and the initial conditions satisfy $\eta_{y,\ell}(0) \in [0, \vartheta_{\eta_y,\ell})$ and $\eta_{\hat{y},\ell}(0) \in [0, \vartheta_{\eta_{\hat{y}},\ell})$. Here,

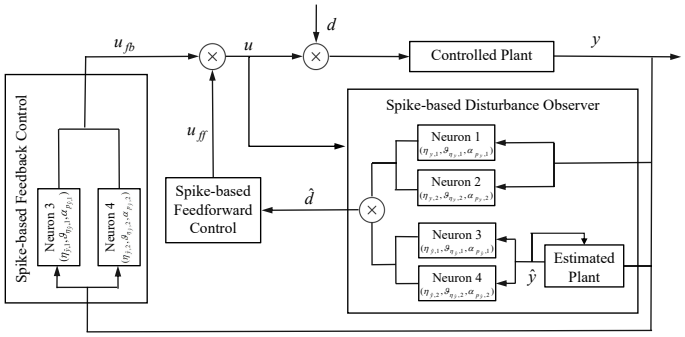

Fig. 1. Architecture diagram of the spike-based disturbance observer and control.

$\vartheta_{\eta_y,\ell},\ \vartheta_{\eta_{\hat{y}},\ell} \in \mathbb{R}_{>0}$ denotes the firing threshold associated with neuron ℓ, and its evolution is governed by the following dynamical equation.

$$\begin{cases} \dot{\vartheta}_{m,\ell}(t) = -\kappa_{m,\ell}\big(\vartheta_{m,\ell}(t) - \bar{\vartheta}_{m,\ell}\big), & t \neq t_{m,k} \\ \vartheta_{m,\ell}(t_{m,k}^+) = \min\Big(\vartheta_{m,\ell}(t_{m,k}^-) + \rho_{m,\ell},\ \vartheta_{m,\ell}^{\max}\Big), & t = t_{m,k} \end{cases} \tag{5}$$

where $\kappa_{m,\ell} > 0$ is the decay rate, $\bar{\vartheta}_{m,\ell} > 0$ is the baseline threshold, $\rho_{m,\ell} > 0$ denotes the adaptation gain. The sequence $\{t_{m,k}\}_{k\in\mathbb{Z}_{>0}}$ represents the spiking instants of η_y and $\eta_{\hat{y}}$, for $\ell \in \{1, 2\}$. Furthermore, for any $t \in \mathbb{R}_{\geq 0}$, the non-negative integers $\ell_{y,\ell_j}(t)$ and $\ell_{\hat{y},\ell_j}(t)$ represent the cumulative number of spikes emitted by neuron ℓ throughout the interval $[0, t]$. $\vartheta_{m,\ell}^{\max}$ denotes the maximum firing threshold. Neuron $\ell \in \{1, 2\}$ emits a spike whenever the condition

$$\eta_{y,\ell}(t) \geq \vartheta_{\eta_y,\ell}(t) \tag{6a}$$

$$\eta_{\hat{y},\ell}(t) \geq \vartheta_{\eta_{\hat{y}},\ell}(t) \tag{6b}$$

is satisfied. Accordingly, the sequence $\{t_{m,\ell_j}\}_{\ell_j\in\mathbb{Z}_{\geq 0}}$, for $\ell \in \{1, 2\}$, is defined as

$$t_{y,0} = 0,\ t_{y,\ell_j+1} := \inf\{t > t_{1,\ell_j} : \eta_{y,\ell}(t) \geq \vartheta_{\eta_y,\ell}(t)\}. \tag{7a}$$

$$t_{\hat{y},0} = 0,\ t_{\hat{y},\ell_j+1} := \inf\{t > t_{2,\ell_j} : \eta_{\hat{y},\ell}(t) \geq \vartheta_{\eta_{\hat{y}},\ell}(t)\}. \tag{7b}$$

The complete sequence of spiking times for the four-neuro is given by $\{t_{m,j}\}_{j\in\mathbb{Z}_{\geq 0}} := \{t_{m,j_1}\}_{j_1\in\mathbb{Z}_{\geq 0}} \cup \{t_{m,j_2}\}_{j_2\in\mathbb{Z}_{\geq 0}}$.

Inspired by the IF neuron model, in which the membrane potential is reset upon reaching a threshold, thus

$$\eta_{m,\ell}(t_{m,\ell_j}^+) = 0, \quad \eta_{m,3-\ell}(t_{2,\ell_j}^+) = \eta_{m,3-\ell}(t_{m,\ell_j}). \tag{8}$$

We now define the spiking input generated by each neuron as, for each $\ell \in \{1, 2\}$, and all $t \in \mathbb{R}_{\geq 0}$,

$$p_{y,\ell}(t) = \sum_{i=1}^{+\infty}(3-2\ell)\alpha_{p_y,\ell}\delta(t - t_{y,\ell_i}) \tag{9a}$$

$$p_{\hat{y},\ell}(t) = \sum_{i=1}^{+\infty}(3-2\ell)\alpha_{p_{\hat{y}},\ell}\delta(t - t_{y,\ell_i}) \tag{9b}$$

and

$$u_{K,\ell}(t) = \sum_{i=1}^{+\infty}(3-2\ell)\alpha_{u\ell}\delta(t - t_{y,\ell_i}). \tag{10}$$

Therefore,

$$p_y(t) = \sum_{i=1}^{+\infty} \alpha_{p_y,1}\delta(t - t_{1,i}) - \sum_{i=1}^{+\infty} \alpha_{p_y,2}\delta(t - t_{2,i}) \quad (11a)$$

$$p_{\hat{y}}(t) = \sum_{i=1}^{+\infty} \alpha_{p_{\hat{y}},1}\delta(t - t_{1,i}) - \sum_{i=1}^{+\infty} \alpha_{p_{\hat{y}},2}\delta(t - t_{2,i}), \quad (11b)$$

and

$$u_{\hat{y},2}(t) = \sum_{i=1}^{+\infty} \alpha_{u_{\hat{y}},1}\delta(t - t_{1,i}) - \sum_{i=1}^{+\infty} \alpha_{u_{\hat{y}},2}\delta(t - t_{2,i}), \quad (12)$$

where $\alpha_{p_y,\ell}$, $\alpha_{p_{\hat{y}},\ell}$ and $\alpha_{u_{\hat{y}},\ell}$ are the amplitude of spiking.

Remark 1. Motivated by the biological fact that neuronal firing thresholds remain strictly positive and bounded due to membrane dynamics and refractory effects [9], it is natural to assume the existence of lower and upper bounds $\vartheta_{m,\ell}^{\min} \leq \vartheta_{m,\ell}(t) \leq \vartheta_{m,\ell}^{\max}$ for all $t \geq 0$. From a control perspective, the strictly positive lower bound $\vartheta_{m,\ell}^{\min}$ guarantees a minimum inter-spike interval and rules out Zeno behavior. A formal analysis of this property is provided in Proposition 1.

Proposition 1. Consider a system of four integrate-and-fire (IF) neurons (1)-(7), where $y(t),\ \hat{y}(t) \in \mathcal{L}_{\mathbb{R}}$ is a signal input to the neurons (4), (6) and (7). The sequence $\{t_{m,\ell_j}\}_{\ell_j \in \mathbb{Z}_{\geq 0}}$ are spiking time. Then, there is a positive constant M_T such that the spiking sequence satisfies a minimum dwell-time condition, i.e., $t_{m,\ell_{j+1}} - t_{m,\ell_j} \geq \vartheta_{m,\ell}^{min}/M_T$, for any $\ell_j \in \mathbb{Z}_{\geq 0}$.

Proof. As y is a locally bounded signal, for any $T \in \mathbb{R}_{\geq 0}$ there is a $M_T \in \mathbb{R}_{>0}$ such that $|y(t)| \leq M_T$ for almost all $t \in [0, T]$. From (4), we have, for all $\ell \in \{1, 2\}$, and all $s \in (t_{y,\ell_i}, t_{y,\ell_i+1})$, $i \in \{1, 2, \ldots, j_\ell(t)\}$,

$$\frac{d}{ds}\eta_{y,\ell}(s) = \max\{0, (3 - 2\ell)y(s)\} \leq M_T$$

Then, for any $s \in (t_{y,\ell_i}, t_{y,\ell_i+1})$,

$$\eta_{y,\ell}(s) \leq \eta_{y,\ell}(t_{y,\ell_i}^+) + M_T(s - t_{\ell,i})$$

Since $\eta_{y,\ell}(t_{y,\ell_i}^+) = 0$ and $\eta_{y,\ell}(t_{y,\ell_{i+1}}) \geq \vartheta_{y,\ell}^{min}$, then

$$t_{y,\ell_{i+1}} - t_{y,\ell_i} \geq \frac{\vartheta_{y,\ell}^{\min}}{M_T}, \quad \forall t \in [0, T]$$

Hence, on any bounded interval $[0, T]$, there cannot be Zeno behavior, which implies either $\ell_i < \infty$ or $t_{y,\ell_i} \to \infty$ as $\ell_i \to \infty$ for all $\ell \in \{1, 2\}$. Similarly, for $t \in [0, T]$

$$t_{\hat{y},\ell_{i+1}} - t_{\hat{y},\ell_i} \geq \frac{\vartheta_{\hat{y},\ell}^{min}}{M_T}$$

The proof is completed. □

Theorem 1. Consider a system of four IF neurons (1)-(7), where $y(t),\ \hat{y}(t) \in \mathcal{L}_{\mathbb{R}}$ is a signal input to the neurons (4), (6) and (7). L satisfies Assumption 3. Then, for any $t \in \mathbb{R}_{\geq 0}$, and each $\ell \in \{1, 2\}$,

$$\left| \int_0^t \max\{0,\ (3 - 2\ell)Ly(s)\} - (3 - 2\ell)p_{y,\ell}(s)\, ds \right| \leq \Psi_{1,\ell},$$

and

$$\left| \int_0^t \max\{0,\ (3 - 2\ell)L\hat{y}(s)\} - (3 - 2\ell)p_{\hat{y},\ell}(s)\, ds \right| \leq \Psi_{2,\ell},$$

with $\Psi_{1,\ell} = L\vartheta_{y,\ell}^{max} + L\ell_i(\max\{|\bar{\vartheta}_{y,\ell} - \frac{\alpha_{p_y,\ell}}{L}|, |\vartheta_{y,\ell}^{max} - \frac{\alpha_{p_y,\ell}}{L}|\})$, $\Psi_{2,\ell} = L\vartheta_{\hat{y},\ell}^{max} + L\ell_i(\max\{|\bar{\vartheta}_{\hat{y},\ell} - \frac{\alpha_{p_{\hat{y}},\ell}}{L}|, |\vartheta_{\hat{y},\ell}^{max} - \frac{\alpha_{p_{\hat{y}},\ell}}{L}|\})$, p_ℓ defined in (11a). Moreover, for any $t \in \mathbb{R}_{\geq 0}$,

$$\left| \int_0^t \psi(s)\, ds \right| \leq L \sum_{\ell=1}^{2} (\vartheta_{y,\ell}^{max} + \vartheta_{\hat{y},\ell}^{max}) + \Psi \quad (13)$$

with $\psi(t) = \max\{0, Ly(s)\} - \max\{0, -Ly(s)\} - \max\{0, L\hat{y}(s)\} + \max\{0, -L\hat{y}(s)\} - p(t) \in \mathbb{R},\ t \in \mathbb{R}_{\geq 0}$, where p is defined in (11a), $\Psi = \sum_{\ell=1}^{2}(L\ell_i(\max\{|\bar{\vartheta}_{y,\ell} - \frac{\alpha_{p_y,\ell}}{L}|, |\vartheta_{y,\ell}^{max} - \frac{\alpha_{p_y,\ell}}{L}|\}) + L\ell_i(\max\{|\bar{\vartheta}_{\hat{y},\ell} - \frac{\alpha_{p_{\hat{y}},\ell}}{L}|, |\vartheta_{\hat{y},1\ell}^{max} - \frac{\alpha_{p_{\hat{y}},\ell}}{L}|\}))$. Moreover, in case $\eta_{y,\ell}(0) = \eta_{\hat{y},\ell}(0) = 0$ and $\ell \in \{1, 2\}$, then

$$\left| \int_0^t \psi(s)\, ds \right| \leq L \sum_{\ell=1}^{2} \max\{\vartheta_{y,\ell}^{max},\ \vartheta_{\hat{y},\ell}^{max}\} + \Psi \quad (14)$$

for any $t \in \mathbb{R}_{\geq 0}$.

The proof of Theorem 1 is provided in the Appendix VIII-A.

Remark 2. Theorem 1 establishes that the IF neuron-generated spike signals $p_{y,\ell}(t)$ and $p_{\hat{y},\ell}(t)$ approximate the observer outputs $Ly(t)$ and $L\hat{y}(t)$ in an integral sense, with a bounded approximation error. This result provides a rigorous justification for replacing continuous-valued observer signals with event-driven spike encoding in the proposed spike-based estimation and control framework.

Corollary 1. Consider the same setup as in Theorem 1. If the control gain K satisfies Assumption 1, then all the integral bounds and inequalities in Theorem 1 hold with L replaced by K.

Proof. The proof of this theorem is similar to that of Theorem 1 and is therefore omitted. □

IV. ISISS PROPERTY FOR DISTURBED SYSTEM

For general nonlinear systems of the form

$$\dot{z} = f(z, v), \quad (15)$$

with $z \in \mathbb{R}^{n_z}$ and $v \in \mathcal{S}^{n_v}$, $n_z, n_v \in \mathbb{Z}_{>0}$, provided that solutions to (15) with $z(0) = z_0 \in \mathbb{R}^{n_z}$ and spiking input $v \in \mathcal{S}^{n_v}$ are well-defined, exist on $\mathbb{R}_{\geq 0}$ and are unique.

Definition 1. *System (15) is* integral spiking-input-to-state stable (iSISS)*, if there are functions $\gamma \in \mathcal{K}$ and $\beta \in \mathcal{KL}$ such that, for any $z(0) = z_0 \in \mathbb{R}^{n_z}$ and all $v \in \mathcal{S}^{n_v}$, the corresponding solution z is defined and satisfies*

$$|z(t)| \leq \beta(|z_0|, t) + \gamma_1(\|v_1\|_\star) + \gamma_2(\|v_2\|_\star) \quad (16)$$

for all $t \in \mathbb{R}_{\geq 0}$. where $\beta(|z_0|, t) := ce^{-\lambda t}|z_0|$, $\|v\|_\star := \sup_{t \in \mathbb{R}_{\geq 0}} \left| \int_0^t v(s)ds \right| < +\infty$, c, λ are positive constants.

In this section, we show that, under the spike-based disturbance estimation and control framework, system 1 is iSISS. The continuous control input is designed as

$$u = K\hat{y} - B^{-1}\hat{d}, \quad (17)$$

where $K \in \mathbb{R}^{n_u \times n_x}$ satisfies the Assumption 1.

Substituting (17) into the original system (1) yields the closed-loop dynamics

$$\begin{aligned}\dot{x}_c &= Ax_c + B(K\hat{y}_c - B^{-1}\hat{d}) + d \\ &= Ax_c + BKC\hat{x}_c + d - \hat{d} \\ &= (A+BKC)x_c + BK(\hat{x}_c - x_c) + d - \hat{d} \\ &= (A+BKC)x_c + Be_{c_x} + e_{c_d}\end{aligned}$$

where x_c denotes the state of closed-loop system, $e_{c_x} = K(\hat{x}_c - x_c)$, $e_{c_d} = d - \hat{d}$.

The spiking control system is as follows:

$$\begin{aligned}\dot{x} &= Ax + Bu + d \\ &= Ax + B(u_K - B^{-1}p) + d \\ &= (A+BKC)x + B(u_K - Kx) + d - p \\ &= (A+BKC)x + Be_x + e_d\end{aligned}$$

where $e_x = u_K - Kx$, $e_d = d - p$.

Let $\tilde{x} = x - x_c$, where $\tilde{x}$ represents the state difference between the two paradigms. We have

$$\dot{\tilde{x}} = \dot{x} - \dot{x}_c = (A+BKC)\tilde{x} + B\tilde{e}_x + \tilde{e}_d$$

where $\widetilde{e}_x = e_x - e_{c_x}$, $\widetilde{e}_d = e_d - e_{c_d}$. Let $\bar{A} = A + BKC \in \mathbb{R}^{n_x \times n_x}$. From Assumption 1, $\bar{A}$ is Hurwitz.

Theorem 2. Consider system (15) with $f(z,v) = Fz + G_1v_1 + G_2v_2$, and $F \in \mathbb{R}^{n_z \times n_z}$ Hurwitz and $G \in \mathbb{R}^{n_z \times n_v}$. Then it is iSISS with $\gamma \in \mathcal{K}$ given by $\gamma_i(s) = \tilde{\gamma}_i s \in \mathcal{K}$, $s \in \mathbb{R}_{\geq 0}$, with $\tilde{\gamma} := \|G_i\| + \int_0^\infty \|Fe^{Fs}G_i\|\, ds \in \mathbb{R}_{\geq 0},\ i = 1, 2$.

The proof of Theorem 2 is provided in the Appendix VIII-B.

Theorem 3. Consider system (1) with $n_u = n_y = 1$. Let u be given by (11a) and (11b) using (4)-(9a) with $\alpha_\ell \in \mathbb{R}_{>0}$ and $\vartheta_{\eta_y,\ell} \in \mathbb{R}_{>0}$, $\ell \in \{1,2\}$, in (7). (9a) such that K, L satisfy Assumption 1 and 3, $\ell \in \{1,2\}$. Then, for any $x(0) = \bar{x}(0) \in \mathbb{R}^{n_x}$, and any $\eta_{y,\ell}(0) \in [0, \vartheta_{\eta_y,\ell})$, $\eta_{\hat{y},\ell}(0) \in [0, \vartheta_{\eta_{\hat{y}},\ell})$, $\ell \in \{1,2\}$, it holds that

$$\begin{aligned}|\tilde{x}(t)| \leq& \gamma_1[\vartheta_{\xi 1} + \vartheta_{\xi 2} + K(M\|e(0)\|e^{-\lambda t} + \gamma\delta)] \\ &+ \gamma_2(\alpha_{y,1} + \alpha_{\hat{y},1} + \alpha_{y,2} + \alpha_{\hat{y},2}).\end{aligned} \tag{18}$$

where $\gamma := \|B\| + \int_0^\infty \|\bar{A}e^{\bar{A}s}B\|ds \in \mathbb{R}_{\geq 0}$. Moreover, if $\eta_1(0) = \eta_2(0) = 0$, then for any $x(0) = \bar{x}(0) = x_0 \in \mathbb{R}^{n_x}$, for all $t \in \mathbb{R}_{\geq 0}$,

$$\begin{aligned}|\tilde{x}(t)| \leq& \gamma_1[\vartheta_{\xi 1} + \vartheta_{\xi 2} + K(M\|e(0)\|e^{-\lambda t} + \gamma\delta)] \\ &+ \gamma_2(\max\{\alpha_{y,1},\ \alpha_{\hat{y},1}\} + \max\{\alpha_{y,2},\ \alpha_{\hat{y},2}\}).\end{aligned} \tag{19}$$

Furthermore,

$$\begin{aligned}\lim_{t\to+\infty} |\tilde{x}(t)| \leq& \gamma_1(\vartheta_{\xi 1} + \vartheta_{\xi 2} + K\gamma\delta) \\ &+ \gamma_2(\max\{\alpha_{y,1},\ \alpha_{\hat{y},1}\} + \max\{\alpha_{y,2},\ \alpha_{\hat{y},2}\}).\end{aligned}$$

The proof of Theorem 3 is provided in the Appendix VIII-C.

This theorem prove the boundedness of the state difference between the two paradigms. Based on Theorem VIII-C, the boundedness of the state x of spiked-based system is proved in Theorem 4.

Theorem 4. Consider system (1) with $n_u = n_y = 1$. Let u be given by (11a) and (11b) using (4)-(9a) with $\alpha_\ell \in \mathbb{R}_{>0}$ and $\vartheta_{\eta_y,\ell} \in \mathbb{R}_{>0}$, $\ell \in \{1,2\}$, in (7). (9a) such that K, L satisfy Assumption 1 and 3, $\ell \in \{1,2\}$. Then, for any $x(0) = \bar{x}(0) \in \mathbb{R}^{n_x}$, and any $\eta_{y,\ell}(0) \in [0, \vartheta_{\eta_y,\ell})$, $\eta_{\hat{y},\ell}(0) \in [0, \vartheta_{\eta_{\hat{y}},\ell})$, $\ell \in \{1,2\}$, it holds that

$$\begin{aligned}|x(t)| \leq& \beta(|x_0,t|) + \gamma_1[\Psi_{2,1} + \Psi_{2,2} + K(M_e\|e(0)\|e^{-\lambda t} \\ &+ \gamma\delta)] + \gamma_2(\alpha_{y,1} + \alpha_{\hat{y},1} + \alpha_{y,2} + \alpha_{\hat{y},2}).\end{aligned} \tag{20}$$

where $\gamma := \|B\| + \int_0^\infty \|\bar{A}e^{\bar{A}s}B\|ds \in \mathbb{R}_{\geq 0}$. Moreover, if $\eta_1(0) = \eta_2(0) = 0$, then for any $x(0) = \bar{x}(0) = x_0 \in \mathbb{R}^{n_x}$, for all $t \in \mathbb{R}_{\geq 0}$,

$$\begin{aligned}|x(t)| \leq& \beta(|x_0,t|) + \gamma_1[\Psi_{2,1} + \Psi_{2,2} + K(M_e\|e(0)\|e^{-\lambda t} \\ &+ \gamma\delta)] + \gamma_2(\max\{\alpha_{y,1},\ \alpha_{\hat{y},1}\} + \max\{\alpha_{y,2},\ \alpha_{\hat{y},2}\}).\end{aligned} \tag{21}$$

Furthermore,

$$\begin{aligned}\lim_{t\to+\infty} |x(t)| \leq& \gamma_1(\Psi_{2,1} + \Psi_{2,2} + K\gamma\delta) \\ &+ \gamma_2(\max\{\alpha_{y,1},\ \alpha_{\hat{y},1}\} + \max\{\alpha_{y,2},\ \alpha_{\hat{y},2}\}).\end{aligned} \tag{22}$$

Proof. Since $\tilde{x} = x - x_c$, we get

$$|x(t)| = |\tilde{x}(t) + x_c(t)| \leq |\tilde{x}(t)| + |x_c(t)|.$$

In view of Assumption 1, $\bar{A}$ is Hurwitz and thus, there exist $c, \lambda \in \mathbb{R}_{>0}$ such that $|x_c(t)| \leq ce^{-\lambda t}|x_c(0)| = \beta(|x_c(0)|, t)$, for all $t \in \mathbb{R}_{\geq 0}$.

The boundedness of the state difference $\tilde{x}$ between the two paradigms, as stated in Theorems 3. Consequently, we obtain (20). Using $x_c(0) = x(0) = x_0 \in \mathbb{R}^{n_x}$, and the bound on $|\tilde{x}|$, we can obtain 21. Since $\lim_{t\to+\infty} \beta(|x_0,t|) = 0$, (22) is obtained. The proof of Theorem 4 is completed. □

Remark 3. Beyond theoretical analysis, the proposed spike-driven framework is compatible with emerging neuromorphic hardware, which has demonstrated potential in event-driven sensing [13] and actuation [14]. While existing hardware-oriented studies often emphasize bio-plausibility, they typically lack formal stability guarantees. In contrast, this work establishes a provably stable spike-driven estimation and control paradigm, providing a foundation for hardware-integrated neuromorphic systems.

V. Generalizations

A. Nonlinear system

Extend system 1 into a nonlinear spiking control system as follows:

$$\dot{z} = g(z) + Bu + d, \qquad y = Cz \tag{23}$$

where $z \in \mathbb{R}$ denotes the state vector with initial condition $z(0) = z_0 \in \mathbb{R}$, $y \in \mathbb{R}$ is the output, and $u \in \mathbb{R}$ represents the (spiking) control input, d denotes the time-varying disturbance. B, $C \in \mathbb{R}$.

Assumption 4. The nonlinear function $g(\cdot)$ is globally Lipschitz. That is, there exists constants M and K such that

$$\|g(x_1) - g(x_2)\| \leq M\|x_1 - x_2\|,\ \forall\ x_1, x_2 \in \mathbb{R}^n. \tag{24}$$

and $M + BKC < 0$.

Theorem 5. Consider system (23), and g satisfies Assumption 4. Assume that there exists an equilibrium point $z^* \in \mathbb{R}$ of the system such that $g(z^*) = 0$. Then, with respect to the equilibrium z^*, the system is iSISS. More precisely, there exist $\beta \in \mathcal{KL}$ and $\gamma_i \in \mathcal{K}$, $i = 1, 2$, such that

$$\|z(t) - z^*\| \leq \beta(\|z(0) - z^*\|, t) + \gamma_1(\|v_1\|_*) + \gamma_2(\|v_2\|_*). \tag{25}$$

The proof of Theorem 5 is provided in the Appendix VIII-D.

B. MIMO system

In previous theorems, we analyzed SISO systems, including both linear and nonlinear cases. We now extend the results to Multiple-Input Multiple-Output (MIMO) systems (2) with $u = (u_1, u_2, \ldots, u_{n_u}) \in \mathbb{R}^{n_u}$, $\hat{y} = (\hat{y}_1, \hat{y}_2, \ldots, \hat{y}_{n_{\hat{y}}}) \in \mathbb{R}^{n_{\hat{y}}}$, $p = (p_1, p_2, \ldots, p_{n_p}) \in \mathbb{R}^{n_p}$ and $n_{\hat{y}} \leq n_u$, $n_{\hat{y}} \leq n_p$. For a MIMO version of Assumption 1 satisfied, to prove a practical stability property, the control input and disturbance observer to emulate is given by

$$u_c = K\hat{y} - B^{-1}\hat{d}, \ \dot{\hat{d}} = L(y - \hat{y}) \tag{26}$$

with $K \in \mathbb{R}^{n_u \times n_{\hat{y}}}$ and $L \in \mathbb{R}^{n_p \times n_e}$,

Each component of the disturbance observer is given by

$$p_i = \sum_{j=1}^{n_e} L_{i,j}(y_j(t) - \hat{y}_j(t)), i \in \{1, 2, \ldots, n_p\}.$$

We can therefore design a network composed of $4n_p * n_e$ IF neurons with dynamics

$$\dot{\eta}^{i,j}_{m,\ell}(t) = \max\{0, (3 - 2\ell)y_j(t)\} \tag{27}$$

with $\eta_{i,j}(0) \in [0, \vartheta^{i,j}_{\eta_y,\ell})$, $\vartheta^{i,j}_{\eta_y,\ell} > 0$, $\ell \in \{1, 2\}$, $i \in \{1, \ldots, n_p\}$, and $j \in \{1, \ldots, n_y\}$. Neuron $\eta_{i,j}$ emits spikes with amplitude $\alpha_{i,j} > 0$ when $\eta^{i,j}_{y,\ell}$ and $\eta^{i,j}_{\hat{y},\ell}$ reach their respective thresholds. The resulting spike train $\{t^i_{m,\ell_j}\}_{\ell_j \in \mathbb{Z}_{\geq 0}}$ is delivered as the input u_i to the system. Similar to Proposition 1, the generated spiking signal p_i emulates $L_i(y_{i,j} - \hat{y}_{i,j})$.

Note that, similarly to Theorem 1, the bound on the emulation error depends on the spikes' amplitudes $\alpha^{i,j}_{p_y,\ell}$, $\alpha^{i,j}_{p_{\hat{y}},\ell} \in \mathbb{R}_{>0}$ and thus can be made arbitrarily small if there is freedom in selecting the thresholds $\vartheta^{i,j}_{\eta_{y_p},\ell}$ and $\vartheta^{i,j}_{\eta_{\hat{y}_p},\ell}$.

VI. Numerical Example

We now consider a linearized model of an unstable batch reactor process. This system is given by (1) with matrices

$$A = \begin{bmatrix} 1.3 & -0.2 & 6.7 & -5.6 \\ -0.5 & -4.2 & 0 & 0.6 \\ 1.0 & 4.1 & -6.6 & 5.8 \\ 0.1 & 4.3 & 1.3 & -2.1 \end{bmatrix}, B = \begin{bmatrix} 0 & 0 \\ 5.6 & 0 \\ 1.1 & -3.1 \\ 1.2 & 0 \end{bmatrix},$$

$$C = \begin{bmatrix} 1 & 0 & 1 & -1 \\ 0 & 1 & 0 & 0 \end{bmatrix}, d_m(t) = \begin{bmatrix} 0.5\sin(0.8t) + 0.3\cos(2t) \\ 0.4\cos(1.2t) + 0.2\sin(3t) \end{bmatrix}.$$

The system is subject to external disturbances, and an ESO in (2) is employed to estimate the lumped disturbance. Under the feedback gain K, the closed-loop matrix $A + BKC$ is Hurwitz, ensuring that Assumption 1 is satisfied. Hence, this MIMO system can be stabilized using the output feedback

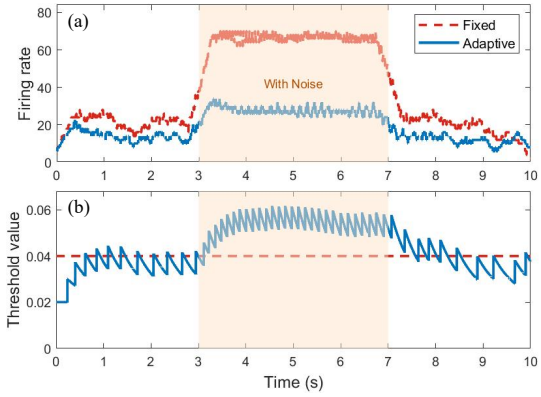

Fig. 2. Comparison of the adaptation properties for fixed and adaptive thresholds in the spike-based disturbance estimate.

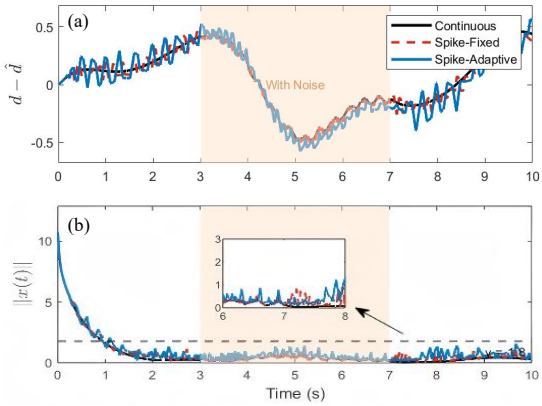

Fig. 3. Comparison of the robust properties for the continuous and spike-based disturbance estimate.

gain $K = \begin{bmatrix} -0.5 & -2 \\ 5 & 0.5 \end{bmatrix}^\top$. The observer gain is chosen as $L = \begin{bmatrix} -1 & -2 & 0.5 & -1 \\ 1 & 0.5 & -1 & 0.5 \end{bmatrix}^\top$, such that $A + LC$ is Hurwitz, which ensures that Assumption 3 holds. Hence, the observer error dynamics are exponentially stable under disturbances.

For the adaptive threshold mechanism, the parameters are selected as: $\bar{\vartheta}_{m,\ell} = 0.02$, $\kappa_{m,\ell} = 2.0$, $\rho_{m,\ell} = 0.01$, $\vartheta^{\max}_{m,\ell} = 0.4$, the fixed threshold $\vartheta_{\text{fixed}} = 0.04$, and the spike amplitude $\alpha_{p_y,\ell} = \alpha_{p_{\hat{y}},\ell} = \alpha_{u_{\hat{y}},\ell} = 0.02$, $\ell = 1, 2$.

A high-frequency noise burst is injected in the interval $[3, 7]$ s. As shown in Fig. 2, during the noise injection, the firing rate of the spike-based ESO with a fixed threshold rapidly increased, reaching 68 spikes/s, whereas the dynamic threshold limited the firing rate to 29 spikes/s, corresponding to only 42.6% of the fixed-threshold case. This clearly demonstrates the adaptation capability of the dynamic threshold. As illustrated in Fig. 3(a), both fixed- and adaptive-threshold spike-based observers achieve comparable disturbance estimation performance, indicating that the spike-based disturbance estimate can accurately capture the injected disturbances, with estimation results close to those obtained by the continuous observer. Furthermore, Fig. 3(b) shows that under the spike-based estimation scheme, the state norm $\|x\|$ converges to a small neighborhood around the origin, verifying the practical

stability and robustness of the proposed approach.

VII. Conclusion

This paper developed a neurally inspired spike-based disturbance estimation and control framework. By incorporating a the SFA mechanism, the framework establishes an intrinsic coupling between update frequency and disturbance dynamics. Theoretically, the practical stability of the closed-loop system is rigorously established, ensuring that both estimation errors and system states remain bounded under external disturbances. Moreover, the proposed approach is further extended to MIMO LTI systems. Numerical simulations further validate that the proposed method achieves precise disturbance compensation and fast convergence. This work demonstrates that the integration of biological spike-firing mechanisms and formal control theory provides a robust and adaptive solution for systems operating in uncertain environments. Future work will focus on extending the proposed framework to uncertain nonlinear systems and exploring hardware implementations, such as memristor-/RRAM-based and analog circuit realizations.

VIII. Appendix

A. Proof of Theorem 1

Proof. According to (7) and (11a), we have

$$\begin{aligned}
&\int_0^t \max\{0,(3-2\ell)Ly(s)\} - (3-2\ell)p_{y,\ell}(s)\,ds\\
=&\int_0^t \max\{0,(3-2\ell)Ly(s)\} - \sum_{i=1}^{+\infty}\alpha_{p,\ell}\delta(s-t_{y,\ell_i})\,ds\\
=&\sum_{i=1}^{\ell_{y,j}(t)}\int_{t^+_{y,\ell_{i-1}}}^{t^+_{y,\ell_i}}\Big[\max\{0,(3-2\ell)Ly(s)\} - \alpha_{p,\ell}\delta(s-t_{y,\ell_i})\Big]\,ds\\
&+\int_{t^+_{y,\ell_{j}(t)}}^{t}\max\{0,(3-2\ell)Ly(s)\}\,ds.
\end{aligned} \tag{28}$$

From (4), (7) and (8), we have that for all $\tilde{t}\in[t_{y,\ell_{i-1}},t_{y,\ell_i})$,

$$\begin{aligned}
\eta_\ell(\tilde{t}) =&\eta_\ell(t^+_{y,\ell_{i-1}}) + \int_{t^+_{y,\ell_{i-1}}}^{\tilde{t}}\max\{0,(3-2\ell)Ly(s)\}ds\\
=&\int_{t^+_{y,\ell_{i-1}}}^{\tilde{t}}\max\{0,(3-2\ell)Ly(s)\}ds.
\end{aligned} \tag{29}$$

From (7) and (29), we have for all $i\in\{2,3,\dots,\ell_{y,j}(t)\}$,

$$\vartheta_{\eta_y,\ell} = \eta_\ell(t^-_{y,\ell_i}) = \int_{t^+_{y,\ell_{i-1}}}^{t^-_{y,\ell_i}}\max\{0,(3-2\ell)Ly(s)\}ds. \tag{30}$$

Since $y(t)\in\mathcal{L}_{\mathbb{R}}$, one has, for any $T_0\in\mathbb{R}_{\geq 0}$,

$$\int_{T_0^-}^{T_0^+}\max\{0,(3-2\ell)Ly(s)\}ds = 0. \tag{31}$$

Thus, from (30) and (31) we have, for all $i\in\{2,3,\dots,\ell_{y,j}(t)\}$

$$L\vartheta_{\eta_y,\ell} = \int_{t^+_{y,\ell_{i-1}}}^{t^+_{y,\ell_i}}\max\{0,(3-2\ell)Ly(s)\}ds. \tag{32}$$

Thus,

$$\begin{aligned}
&\int_{t^+_{y,\ell_{i-1}}}^{t^+_{y,\ell_i}}(\max\{0,(3-2\ell)Ly(s)\} - \alpha_{p_y,\ell}\delta(s-t_{y,\ell_i}))ds\\
=&L\vartheta_{\eta_y,\ell}(t_{y,\ell_i}) - \alpha_{p_y,\ell}.
\end{aligned} \tag{33}$$

Using (28), (33) becomes

$$\begin{aligned}
&\int_0^t \max\{0,(3-2\ell)Ly(s)\} - (3-2\ell)p_{y,\ell}(s)ds\\
&=\int_{t^+_{\ell,0}}^{t^+_{\ell,1}}(\max\{0,(3-2\ell)Ly(s)\} - \vartheta_{\eta_y,\ell}\delta(s-t_{\ell,1}))ds\\
&\quad+\int_{t^+_{\ell,\ell_{y,j}(t)}}^{t}\max\{0,(3-2\ell)Ly(s)\}ds\\
&\quad+\sum_{j=0}^{\ell_i}L\vartheta_{\eta_y,\ell}(t_{y,\ell_j}) - \ell_i\alpha_{p_y,\ell}.
\end{aligned} \tag{34}$$

From (29) with $i=1$ and (34), we obtain, for all $t\in\mathbb{R}_{\geq 0}$,

$$\begin{aligned}
&\int_0^t \max\{0,(3-2\ell)Ly(s)\} - (3-2\ell)p_{y,\ell}(s)ds\\
&=L(-\eta_{y,\ell}(0)+\eta_{y,\ell}(t)) + \sum_{j=0}^{\ell_i}L\vartheta_{\eta_y,\ell}(t_{y,\ell_j}) - \ell_i\alpha_{p_y,\ell}\\
&=L(-\eta_{y,\ell}(0)+\eta_{y,\ell}(t)) + L\ell_i\Big(\frac{1}{\ell_i}\sum_{j=0}^{\ell_i}\vartheta_{\eta_y,\ell}(t_{y,\ell_j}) - \frac{\alpha_{p_y,\ell}}{L}\Big).
\end{aligned} \tag{35}$$

Moreover, from (5) and (6), we have $\eta_{y,\ell}(t)\in[0,\vartheta_{y,max}]$ for all $t\in\mathbb{R}_{\geq 0}$. We can conclude that, for all $t\in\mathbb{R}_{\geq 0}$, $\ell\in\{1,2\}$, $L(-\eta_{y,\ell}(0)+\eta_{y,\ell}(t))\in[-L\vartheta^{max}_{y,\ell}, L\vartheta^{max}_{y,\ell}]$. Since $\bar{\vartheta}_{y,\ell}\leq\frac{1}{\ell_i}\sum_{j=0}^{\ell_i}\vartheta_{\eta_y,\ell}(t_{y,\ell_j})\leq\vartheta^{max}_{y,\ell}$ which implies,

$$\begin{aligned}
&\left|\int_0^t \max\{0,(3-2\ell)Ly(s)\} - (3-2\ell)p_{y,\ell}(s)ds\right|\\
&\leq L\vartheta^{max}_{y,\ell} + L\ell_i(\max\{|\bar{\vartheta}_{y,\ell} - \frac{\alpha_{p_y,\ell}}{L}|, |\vartheta^{max}_{y,\ell} - \frac{\alpha_{p_y,\ell}}{L}|\}).
\end{aligned} \tag{36}$$

Similarly, we have

$$\begin{aligned}
&\left|\int_0^t \max\{0,(3-2\ell)L\hat{y}(s)\} - (3-2\ell)p_{\hat{y},\ell}(s)ds\right|\\
&\leq L\vartheta^{max}_{\hat{y},\ell} + L\ell_i(\max\{|\bar{\vartheta}_{\hat{y},\ell} - \frac{\alpha_{p_{\hat{y}},\ell}}{L}|, |\vartheta^{max}_{\hat{y},\ell} - \frac{\alpha_{p_{\hat{y}},\ell}}{L}|\}).
\end{aligned} \tag{37}$$

This concludes the first part of the proof. We now prove the second part of Theorem 1.

From (29), similarly to (35), we obtain, for all $t\in\mathbb{R}_{\geq 0}$,

$$\begin{aligned}
&\int_0^t \psi(s)ds\\
&=L(-\eta_{y,1}(0)+\eta_{y,1}(t)) + L\ell_i\Big(\frac{1}{\ell_i}\sum_{j=0}^{\ell_i}\vartheta_{\eta_y,1}(t_{y,\ell_j}) - \frac{\alpha_{p_y,1}}{L}\Big)\\
&-L(-\eta_{y,2}(0)+\eta_{y,2}(t)) - L\ell_i\Big(\frac{1}{\ell_i}\sum_{j=0}^{\ell_i}\vartheta_{\eta_y,1}(t_{y,\ell_j}) - \frac{\alpha_{p_y,2}}{L}\Big)
\end{aligned}$$

$$- L(-\eta_{\hat{y},1}(0)+\eta_{\hat{y},1}(t)) - L\ell_i(\frac{1}{\ell_i}\sum_{j=0}^{\ell_i}\vartheta_{\eta_{\hat{y},1}}(t_{y,\ell_j}) - \frac{\alpha_{p_{\hat{y}},1}}{L})$$
$$+ L(-\eta_{\hat{y},2}(0)+\eta_{\hat{y},2}(t)) + L\ell_i(\frac{1}{\ell_i}\sum_{j=0}^{\ell_i}\vartheta_{\eta_{\hat{y},2}}(t_{y,\ell_j}) - \frac{\alpha_{p_{\hat{y}},2}}{L}) \tag{38}$$

Similar to (36) and (37), we have

$$\left|\int_0^t \psi(s)ds\right| \le L\sum_{\ell=1}^{2}(\vartheta_{y,\ell}^{max}+\vartheta_{\hat{y},\ell}^{max}) + \Psi. \tag{39}$$

Since

$$\begin{aligned}&|L\eta_{y,1}(t) - L\eta_{y,2}(t) - L\eta_{\hat{y},1}(t) + L\eta_{\hat{y},2}(t)|\\ \le& L|\eta_{y,1}(t)-\eta_{\hat{y},1}(t)| + L|\eta_{y,2}(t)-\eta_{\hat{y},2}(t)|\\ \le& L\max\{\vartheta_{y,1}^{max},\ \vartheta_{\hat{y},1}^{max}\} + L\max\{\vartheta_{y,2}^{max},\ \vartheta_{\hat{y},2}^{max}\}\end{aligned}$$

Following similar steps as in (38)-(39) and considering the case $\eta_{y,\ell}(0)=0$, $\ell\in\{1,2\}$, we have

$$\left|\int_0^t \psi(s)ds\right| \le L\left|\eta_{y,1}(t)-\eta_{y,2}(t)-\eta_{\hat{y},1}(t)+\eta_{\hat{y},2}(t)\right| + \Psi$$
$$\le L\max\{\vartheta_{y,1}^{max},\ \vartheta_{\hat{y},1}^{max}\} + L\max\{\vartheta_{y,2}^{max},\ \vartheta_{\hat{y},2}^{max}\} + \Psi.$$

This completes the proof of Theorem 1. □

B. Proof of Theorem 2

Proof. By solving the differential equation in (15), we have

$$z(t) = e^{Ft}z_0 + \int_0^t e^{F(t-s)}[G_1v_1(s)+G_2v_2(s)]ds. \tag{40}$$

By introducing the notation $h_i(\theta) := e^{F\theta}G_i \in \mathbb{R}^{n\times m}$, for all $\theta\in\mathbb{R}$, the integral term in (40) can be written as

$$\int_0^t h_2(t-s)v_2(s)ds = \sum_{i=1}^{j(t)}\left(\int_{t_{i-1}^+}^{t_i^-} h_2(t-s)v_2(s)ds + \int_{t_i^-}^{t_i^+} h_2(t-s)v_2(s)ds\right) + \int_{t_{j(t)}^+}^{t} h_2(t-s)v_2(s)ds, \tag{41}$$

where $j(t)\in\mathbb{Z}_{\ge0}$ counts spikes up to time t, and t_i is the i-th spike instant. $i\in\{1,2,\dots,j(t)\}$. We now consider the three integrals in (41) separately. We first consider $\int_{t_{i-1}^+}^{t_i^-} h_2(t-s)v_2(s)ds$. Since $h_2(t-s)$ is continuous for all $t,s\in\mathbb{R}_{\ge0}$ with $s\le t$ and v_k is integrable for all $s\in[t_{i-1}^+, t_i^-]$, we can apply the integration by parts and, recalling that $h_2(t-t_i) = h(t-t_i^+) = h(t-t_i^-)$ for all $i\in\{1,2,\dots,j(t)\}$, we obtain

$$\begin{aligned}\int_{t_{i-1}^+}^{t_i^-} h_2(t-s)v_2(s)ds =& h_2(t-t_i)\int_0^{t_i^-} v_2(\theta)d\theta - h_2(t-t_{i-1})\int_0^{t_{i-1}^+} v_2(\theta)d\theta\\ &- \int_{t_{i-1}^+}^{t_i^-}\frac{d}{ds}(h_2(t-s))\int_0^s v_2(\theta)d\theta ds.\end{aligned} \tag{42}$$

Similarly, using the integration by parts the last integral in (41) can be written as,

$$\begin{aligned}&\int_{t_{j(t)}^+}^{t} h_2(t-s)v_2(s)ds\\ &= h_2(0)\int_0^t v_2(\theta)d\theta - h(t-t_{j(t)})\int_0^t v_2(\theta)d\theta ds.\end{aligned} \tag{43}$$

$v_2(t) := \sum_{i=1}^{\infty}\Theta_i\delta(t-t_i)$ with $t\in\mathbb{R}_{\ge0}$ and using the definition of the Dirac delta function, we have

$$\begin{aligned}\int_{t_i^-}^{t_i^+} h_2(t-s)v_2(s)ds =& \int_{t_i^-}^{t_i^+} h_2(t-s)\Theta_i\delta(s-t_i)ds\\ =& h_2(t-t_i)\Theta_i.\end{aligned} \tag{44}$$

From (41) - (44), we obtain

$$\begin{aligned}&\int_0^t h_2(t-s)v_2(s)ds\\ &= \sum_{i=1}^{j(t)}\Bigg(h_2(t-t_i)\int_0^{t_i^-} v_2(\theta)d\theta - h_2(t-t_{i-1})\times\\ &\int_0^{t_{i-1}^+} v_2(\theta)d\theta - \int_{t_{i-1}^+}^{t_i^-}\frac{d}{ds}(h_2(t-s))\int_0^s v_2(\theta)d\theta ds\\ &+h_2(t-t_i)\Theta_i\Bigg) + h_2(0)\int_0^t v_2(\theta)d\theta - h(t-t_{j(t)})\times\\ &\int_0^{t_{j(t)}^+} v_2(\theta)d\theta - \int_{t_{j(t)}^+}^{t}\frac{d}{ds}(h_2(t-s))\int_0^s v_2(\theta)d\theta ds.\end{aligned} \tag{45}$$

In addition, we have $\int_{t_i^-}^{t_i^+}\frac{d}{ds}(h_2(t-s))\int_0^s v_2(\theta)d\theta ds = 0$, for all $i\in\{1,2,\dots,j(t)\}$ and thus, by adding $\sum_{i=1}^{j(t)}\int_{t_i^-}^{t_i^+}\frac{d}{ds}(h_2(t-s))\int_0^s v_2(\theta)d\theta ds = 0$, we have

$$\begin{aligned}&\sum_{i=1}^{j(t)}\int_{t_{i-1}^+}^{t_i^-}\frac{d}{ds}(h_2(t-s))\int_0^s v_2(\theta)d\theta ds\\ &\quad+\int_{t_{j(t)}^+}^{t}\frac{d}{ds}(h_2(t-s))\int_0^s v_2(\theta)d\theta ds\\ &= \int_0^t\frac{d}{ds}(h_2(t-s))\int_0^s v_2(\theta)d\theta ds.\end{aligned} \tag{46}$$

Consequently,

$$\begin{aligned}&\int_0^t h_2(t-s)v_2(s)ds\\ &= h_2(0)\int_0^t v_2(\theta)d\theta - \int_0^t\frac{d}{ds}(h_2(t-s))\int_0^s v_2(\theta)d\theta ds\\ &\quad+\sum_{i=1}^{j(t)}\Bigg(h_2(t-t_i)\int_0^{t_i^-} v_2(\theta)d\theta - h_2(t-t_{i-1})\times\\ &\int_0^{t_{i-1}^+} v_2(\theta)d\theta + h_2(t-t_i)\Theta_i\Bigg) - h(t-t_{j(t)})\int_0^{t_{j(t)}^+} v_2(\theta)d\theta\\ &= h_2(0)\int_0^t v_2(\theta)d\theta - \int_0^t\frac{d}{ds}(h_2(t-s))\int_0^s v_2(\theta)d\theta ds\\ &\quad- h(t-t_0)\int_0^{t_0^+} v_2(\theta)d\theta + \sum_{i=1}^{j(t)} h_2(t-t_i)\times\end{aligned}$$

$$\left(\int_0^{t_i^-} v_2(\theta)d\theta - \int_0^{t_{i-1}^+} v_2(\theta)d\theta + \Theta_i\right)$$
$$= h_2(0)\int_0^t v_2(\theta)d\theta - \int_0^t \frac{d}{ds}(h_2(t-s))\int_0^s v_2(\theta)d\theta ds - h(t-t_0)\int_0^{t_0^+} v_2(\theta)d\theta + \sum_{i=1}^{j(t)} h_2(t-t_i)\left(-\int_{t_{i-1}^+}^{t_i^-} v_2(\theta)d\theta + \Theta_i\right). \quad (47)$$

Since $v \in \mathcal{S}$ and $t_0 = 0$ is not a spiking time, $h(t-t_0)\int_0^{t_0^+} v_2(\theta)d\theta = 0$. Thus,

$$\begin{aligned}
&\int_0^t h_2(t-s)v_2(s)ds \\
&= h_2(0)\int_0^t v_2(\theta)d\theta - \int_0^t \frac{d}{ds}(h_2(t-s))\int_0^s v_2(\theta)d\theta ds \\
&\quad + \sum_{i=1}^{j(t)} h_2(t-t_i) - \int_{t_{i-1}^+}^{t_i^-} \Theta_i\delta(\theta-t_i)d\theta + \Theta_i \\
&= h_2(0)\int_0^t v_2(\theta)d\theta - \int_0^t \frac{d}{ds}(h_2(t-s))\int_0^s v_2(\theta)d\theta ds.
\end{aligned}$$

Similarly,

$$\int_0^t h_1(t-s)v_1(s)ds = h_1(0)\int_0^t v_1(\theta)d\theta - \int_0^t \frac{d}{ds}(h_1(t-s))\int_0^s v_1(\theta)d\theta ds. \quad (48)$$

Consequently, from (40), we have

$$\begin{aligned}
z(t) &= e^{Ft}z_0 + \int_0^t e^{F(t-s)}(G_1v_1(s) + G_2v_2(s))ds \\
&= e^{Ft}z_0 + \left(h_1(0)\int_0^t v_1(\theta)d\theta - \int_0^t \frac{d}{ds}(h_1(t-s))\times \int_0^s v_1(\theta)d\theta ds\right) + \left(h_2(0)\int_0^t v_2(\theta)d\theta - \int_0^t \frac{d}{ds}(h_2(t-s))\times\int_0^s v_2(\theta)d\theta ds\right). \quad (49)
\end{aligned}$$

By the definition of $h_i(t-s)$, one has $h_i(0) = G_i$ and $\frac{d}{ds}(h_i(t-s)) = -Fe^{F(t-s)}G_i \in \mathbb{R}^{n\times m}$ for all $t, s \in \mathbb{R}_{\geq 0}$ with $s \leq t$, and thus, from (49), we obtain, for all $t \geq 0$,

$$z(t) = e^{Ft}z_0 + G_1\int_0^t v_1(\theta)d\theta + G_2\int_0^t v_2(\theta)d\theta + \int_0^t Fe^{F(t-s)}G_1\int_0^s v_1(\theta)d\theta ds + \int_0^t Fe^{F(t-s)}G_2\int_0^s v_2(\theta)d\theta ds.$$

Using the triangular inequality, for all $t \in \mathbb{R}_{\geq 0}$,

$$\begin{aligned}
|z(t)| &= \left|e^{Ft}z_0 + G_1\int_0^t v_1(\theta)d\theta + G_2\int_0^t v_2(\theta)d\theta + \int_0^t Fe^{F(t-s)}G_1\int_0^s v_1(\theta)d\theta ds + \int_0^t Fe^{F(t-s)}G_2\int_0^s v_2(\theta)d\theta ds\right| \\
&\leq \left|e^{Ft}z_0\right| + \left|G_1\int_0^t v_1(\theta)d\theta\right| + \left|G_2\int_0^t v_2(\theta)d\theta\right| + \left|\int_0^t Fe^{F(t-s)}G_1\int_0^s v_1(\theta)d\theta ds\right| + \left|\int_0^t Fe^{F(t-s)}G_2\int_0^s v_2(\theta)d\theta ds\right| \\
&\leq \left|e^{Ft}z_0\right| + \|G_1\|\,\|v_1\|_* + \int_0^t \left\|Fe^{F(t-s)}G_1\right\|\int_0^s |v_1(\theta)|d\theta ds \\
&\quad + \|G_2\|\,\|v_2\|_* + \int_0^t \left\|Fe^{F(t-s)}G_2\right\|\int_0^s |v_2(\theta)|d\theta ds \\
&\leq \left|e^{Ft}z_0\right| + \|G_1\|\,\|v_1\|_* + \int_0^\infty \left\|Fe^{Fs}G\right\| ds\|v_1\|_* \\
&\quad + \|G_2\|\,\|v_2\|_* + \int_0^\infty \left\|Fe^{Fs}G\right\| ds\|v_2\|_*.
\end{aligned}$$

Since F is Hurwitz, there exist $c, \lambda \in \mathbb{R}_{>0}$ such that $\left|e^{Ft}z_0\right| \leq ce^{-\lambda t}|z_0|$. Thus,

$$\begin{aligned}
|z(t)| &\leq ce^{-\lambda t}|z_0| + \left(\|G_1\| + \int_0^\infty \left\|Fe^{Fs}G_1\right\| ds\right)\|v_1\|_* + \left(\|G_2\| + \int_0^\infty \left\|Fe^{Fs}G_2\right\| ds\right)\|v_2\|_* \\
&= \beta(|z_0|, t) + \gamma_1\|v_1\|_* + \gamma_2\|v_2\|_*.
\end{aligned}$$

Note that $\int_0^\infty \left\|Fe^{Fs}G_i\right\| ds$ is finite since F is Hurwitz. This completes the proof of Theorem 2. □

C. Proof of the Theorem 3

Proof. Since $x(0) = x_c(0)$, it holds that $\tilde{x}(0) = 0$. From Theorem 2, we obtain, for all $t \in \mathbb{R}_{\geq 0}$,

$$\begin{aligned}
|\tilde{x}(t)| &\leq \left(\|B\| + \int_0^\infty \|\bar{A}e^{\bar{A}s}B\|ds\right)\|\widetilde{e}_x\|_\star + \left(1 + \int_0^\infty \|\bar{A}e^{\bar{A}s}\|ds\right)\|\widetilde{e}_d\|_\star \\
&= \gamma_1\|\widetilde{e}_x\|_\star + \gamma_2\|\widetilde{e}_d\|_\star. \quad (50)
\end{aligned}$$

From Corollary 1 and (3), we have

$$\begin{aligned}
|\tilde{e}_x| &= |e_x - e_{c_x}| \\
&= |u_K - K\hat{y} - K(\hat{x}_c - x_c)| \\
&\leq |u_K - K\hat{y}| + K\,|\hat{x}_c - x_c| \\
&\leq \vartheta_{\xi 1} + \vartheta_{\xi 2} + K(M_e e^{-\lambda t}\|e(0)\| + \gamma \sup_{0\leq s\leq t}\|\dot{d}(s)\|)
\end{aligned}$$

which implies

$$\|\tilde{e}_x\|_\star \leq \vartheta_{\xi 1} + \vartheta_{\xi 2} + K(M_e e^{-\lambda t}\|e(0)\| + \gamma \sup_{0\leq s\leq t}\|\dot{d}(s)\|).$$

Since $\tilde{e}_d = e_d - e_{c_d} = p - \hat{d}$, it follows from Theorem 1 that

$$\|\tilde{e}_d\|_\star \leq \gamma_2(\alpha_{y,1} + \alpha_{\hat{y},1} + \alpha_{y,2} + \alpha_{\hat{y},2}).$$

Therefore,

$$|\tilde{x}(t)| \leq \gamma_1[\vartheta_{\xi 1} + \vartheta_{\xi 2} + K(M_e e^{-\lambda t}\|e(0)\| + \gamma \sup_{0\leq s\leq t}\|\dot{d}(s)\|)]$$

$$
\begin{aligned}
&+\gamma_2(\alpha_{y,1}+\alpha_{\hat{y},1}+\alpha_{y,2}+\alpha_{\hat{y},2})\\
\le&\gamma_1[\vartheta_{\xi 1}+\vartheta_{\xi 2}+K(M_e\|e(0)\|+\gamma\delta)]\\
&+\gamma_2(\alpha_{y,1}+\alpha_{\hat{y},1}+\alpha_{y,2}+\alpha_{\hat{y},2}). \qquad (51)
\end{aligned}
$$

Specially, if $\eta_{y,\ell}(0)=\eta_{\hat{y},\ell}(0)=0$, from (13) and (51), we have

$$
\begin{aligned}
|\tilde{x}(t)|\le&\gamma_1[\vartheta_{\xi 1}+\vartheta_{\xi 2}+K(M_e\|e(0)\|+\gamma\delta)]\\
&+\gamma_2(\max\{\alpha_{y,1},\ \alpha_{\hat{y},1}\}+\max\{\alpha_{y,2},\ \alpha_{\hat{y},2}\}). \qquad (52)
\end{aligned}
$$

Moreover, from (52), when $t\to+\infty$, we have

$$
\begin{aligned}
\lim_{t\to+\infty}|\tilde{x}(t)|\le&\gamma_1(\vartheta_{\xi 1}+\vartheta_{\xi 2}+K\gamma\delta)\\
&+\gamma_2(\max\{\alpha_{y,1},\ \alpha_{\hat{y},1}\}+\max\{\alpha_{y,2},\ \alpha_{\hat{y},2}\}).
\end{aligned}
$$

This concludes the proof. □

D. Proof of the Theorem 5

Proof. Introduce the shifted state $x:=z-z^*$. Then $z=x+z^*$ and $\dot{x}=\dot{z}$. Hence, the system can be rewritten as

$$\dot{x}=g(x+z^*)+G_1v_1+G_2v_2.$$

Define the shifted nonlinearity

$$\tilde{g}(x):=g(x+z^*)-g(z^*).$$

Since $g(z^*)=0$, it follows that $\tilde{g}(x)=g(x+z^*)$, and clearly $\tilde{g}(0)=0$. Therefore, the transformed system becomes

$$\dot{x}=\tilde{g}(x)+G_1v_1+G_2v_2.$$

Moreover, since g satisfies Assumption 4, we have

$$\|\tilde{g}(x_1)-\tilde{g}(x_2)\|=\|g(x_1+z^*)-g(x_2+z^*)\|\le M\|x_1-x_2\|$$

for all $x_1,x_2\in\mathbb{R}^{n_z}$. In particular, taking $x_2=0$ and using $\tilde{g}(0)=0$, we obtain

$$-Mx\le\tilde{g}(x)\le Mx,\qquad \forall x\in\mathbb{R}^{n_z}.$$

Consider the following upper bounding system:

$$\dot{x}_{up}=Mx_{up}+G_1v_1+G_2v_2.$$

According to the Assumption 4, and similarily to the proof Theorem3 and Theorem 4, we have

$$
\begin{aligned}
|x_{up}(t)|\le&\beta(|x_0,t|)+\gamma_2(\alpha_{y,1}+\alpha_{\hat{y},1}+\alpha_{y,2}+\alpha_{\hat{y},2})\\
&+\gamma_1[\Psi_{2,1}+\Psi_{2,2}+K(M_e\|e(0)\|e^{(M+BKC)t}+\gamma\delta)].
\end{aligned}
$$

Consider the following lower bounding system:

$$\dot{x}_{low}=-Mx_{low}+G_1v_1+G_2v_2$$

similarly, we have

$$
\begin{aligned}
|x_{low}(t)|\le&\beta(|x_0,t|)+\gamma_2(\alpha_{y,1}+\alpha_{\hat{y},1}+\alpha_{y,2}+\alpha_{\hat{y},2})\\
&+\gamma_1[\Psi_{2,1}+\Psi_{2,2}+K(M_e\|e(0)\|e^{(-M+BKC)t}+\gamma\delta)].
\end{aligned}
$$

Hence, according the comparison principle, one has

$$x_{low}(t)\le x(t)\le x_{up}(t).$$

Since $-M+BK<M+BK$, hence, $|x(t)|\le|x_{up}(t)|$. Recalling that $x=z-z^*$, yields

$$
\begin{aligned}
\|z(t)-z^*\|\le&\beta(|x_0,t|)+\gamma_2(\alpha_{y,1}+\alpha_{\hat{y},1}+\alpha_{y,2}+\alpha_{\hat{y},2})\\
&+\gamma_1[\Psi_{2,1}+\Psi_{2,2}+K(M_e\|e(0)\|e^{(M+BKC)t}+\gamma\delta)].
\end{aligned}
$$

Hence,

$$
\begin{aligned}
\|z(t)\|\le&z^*+\beta(|x_0,t|)+\gamma_2(\alpha_{y,1}+\alpha_{\hat{y},1}+\alpha_{y,2}+\alpha_{\hat{y},2})\\
&+\gamma_1[\Psi_{2,1}+\Psi_{2,2}+K(M_e\|e(0)\|e^{(M+BKC)t}+\gamma\delta)].
\end{aligned}
$$

We conclude that the system is iSISS with respect to the equilibrium z^*. Finally, since $\beta(r,t)=ce^{-\lambda t}r$ is of class $\mathcal{KL}$ and each $\gamma_i(s)=\tilde{\gamma}_i s$ is of class $\mathcal{K}$, the proof is complete. □

REFERENCES

[1] R. Sepulchre, "Spiking control systems," *Proc. IEEE*, vol. 110, no. 5, pp. 577–589, 2022.

[2] J. Rosito, E. Petri, E. Steur, and W. Heemels, "Design, modelling and analysis of a bio-inspired spiking temperature regulator," in *Proc. IEEE Conf. Decis. Control (CDC)*. IEEE, 2025, pp. 39–44.

[3] C. Zhang, C. Wang, W. Pan, and C. Della Santina, "Spikingsoft: A spiking neuron controller for bio-inspired locomotion with soft snake robots," in *Proc. IEEE Int. Conf. Soft Robot. (RoboSoft)*. IEEE, 2025, pp. 1–8.

[4] L. Mendolia *et al.*, "A neuromodulable current-mode silicon neuron for robust and adaptive neuromorphic systems," *arXiv*, 2025.

[5] A. Cecconi, M. Bin, R. Sepulchre, and L. Marconi, "Event disturbance rejection: a case study," *IFAC-PapersOnLine*, vol. 59, no. 19, pp. 262–267, 2025.

[6] E. Petri, K. J. Scheres, E. Steur *et al.*, "Emulation-based neuromorphic control for the stabilization of LTI systems," *arXiv preprint arXiv:2511.11875*, 2025.

[7] L. Eilers, J. Stapmanns, C. Dias, and J.-P. Pfister, "On the stability of event-based control with neuronal dynamics," *arXiv preprint arXiv:2511.18015*, 2025.

[8] E. Petri, K. J. A. Scheres, E. Steur, and W. P. M. H. Heemels, "Analysis of a simple neuromorphic controller for linear systems," in *Proc. IEEE Conf. Decis. Control (CDC)*, 2024, pp. 8578–8583.

[9] S. M. Kang *et al.*, "How to build a memristive integrate-and-fire model for spiking neuronal signal generation," *IEEE Trans. Circuits Syst. I, Regul. Pap.*, vol. 68, no. 12, pp. 4837–4850, 2021.

[10] L. Guo and W. Chen, "Disturbance attenuation and rejection for systems with nonlinearity via dobc approach," *Int. J. Robust Nonlinear Control*, vol. 15, no. 3, pp. 109–125, 2005.

[11] W.-H. Chen, J. Yang, L. Guo, and S. Li, "Disturbance-observer-based control and related methods: An overview," *IEEE Trans. Ind. Electron.*, vol. 63, no. 2, pp. 1083–1095, 2015.

[12] R. Azouz and C. M. Gray, "Dynamic spike threshold reveals a mechanism for synaptic coincidence detection in cortical neurons in vivo," *Proc. Natl. Acad. Sci. U.S.A.*, vol. 97, no. 14, pp. 8110–8115, 2000.

[13] Y. Xiao *et al.*, "Bio-plausible reconfigurable spiking neuron for neuromorphic computing," *Sci. Adv.*, vol. 11, no. 6, p. eadr6733, 2025.

[14] Y. Yang *et al.*, "Firing feature-driven neural circuits with scalable memristive neurons for robotic obstacle avoidance," *Nat. Commun.*, vol. 15, no. 1, p. 4318, 2024.